PAN
ARCHIVES OF ACOUSTICS
Vol. **44**, No. 2, pp. 259–265 (2019)
DOI: 10.24425/aoa.2019.128489

An Improved MSA Model for Evaluating the Sound Transmission Loss of a Rectangular Plate for Diffuse Field Incidence

Myong-Jin KIM*, Kyong-Su WON, Chol-Su RI

Department of Physics
Kim Il Sung University
Pyongyang, Democratic People's Republic of Korea
*Corresponding Author e-mail: mj_kim7093@163.com

(*received September 30, 2018; accepted February 15, 2019*)

This paper presents an approximate analytical model for estimating the transmission loss (TL) of a finite rectangular plate in the low frequency range, which is based on the modal summation approach (MSA) taking into account the modal radiation impedance and fluid loading. The mode-dependent radiation resistance is calculated using the Rayleigh integral. The fluid loading is taken into account through the natural frequency modified by the added mass. The results are compared with the ones of Statistical Energy Analysis (SEA) coupled with FEM and FEM coupled with BEM. In addition, the effects of the various vibration modes and the fluid loading on TL, and a way for reducing the calculation time are discussed.

Keywords: transmission loss; low frequency range; natural vibration mode; diffuse field incidence.

1. Introduction

A thin rectangular plate is an important component of the buildings as well as the vehicles such as a metro car. Therefore, it is the base for predicting the total sound insulation of the structure to precisely evaluate the transparency of the plate.

The various models and formulas for TL (Vigran, 2008; Fahy, 1995; Callister *et al.*, 1999; Sharp, 1978) were mostly derived based on approximations where the plate was infinite and neglected the effect of the natural vibration modes of the plate. This often leads to the unacceptable discrepancies (over 20 dB) between theories and the practice (Bruneau, 2006). In many cases, the plates can be compared to their flexural wavelengths in the low frequency range, resulting in the distinct effect of the natural vibration modes, so the natural mode of the plate should be considered in this range.

The modal summation approach (MSA) (Xie *et al.*, 2005; Fahy, Gardonio, 2006; Putra, Thompson, 2010) is a good approximation for the acoustic transparency of finite walls, but it is only well suited in the low frequency range due to the computing cost. If the modal density is high in the range of interest, Statistical Energy Analysis should be applied. On the other hand, for low modal density the methods such as FEM and BEM (Sgard *et al.*, 2000) may be applied.

Kozien (2005, 2009) conducted a theoretical study to evaluate the sound radiated by a deterministically vibrating surface while reducing the computing consumption by using a hybrid method that combines FEM and the acoustic intensity vector method, and then generalized the method for the randomly vibrating one with the amplitude described by a probability density function.

The radiation impedance is one of the important factors in the prediction of sound transmission. Frequency- and area-independence of the radiation impedance in an infinite panel- causes the inherent discrepancy with experiment results.

Based on the Rayleigh integral, the sound pressure was calculated as well as the intensity in the far field from a simply supported plate with the velocity $u_z(x, y)$ (Wallace, 1972). By integrating the intensity over a hemisphere over the plate vibrating in a given mode, the radiated power and thereby the radiation factor by definition were derived (Vigran, 2008). In this paper, these results will be used for our calculation of the radiation resistance and specific acoustic impedance below. Besides, several methods (Leppington *et al.*, 1982; Andresen, 1999) for de-

termining the radiation efficiency and various theories (Sedov, 1964; 1990) for transmission of sound waves through finite plates were developed.

Most of the classical theories have been developed assuming light fluid loading, so that the plate response is not affected by the surrounding environment, which acts as an added mass and also provides the radiation damping. Loading by fluid may significantly lower the natural frequencies of flat plates, the effect of which is decreased with increasing the modal order (Arenas, 2003). In the past, the effective surface mass density, fluid loaded resonance frequency, and effective loss factor were suggested (Zhang *et al.*, 2003).

In originally formulated MSA (Bruneau, 2006) loading of the plate by the surrounding fluid is ignored for air and it is assumed that the specific acoustic impedance is independent of mode, resulting in considerable errors.

In this paper, an approximate analytical model, taking into account loading of the plate by the surrounding medium, radiation losses is presented. The results of computations for the diffuse field transmission loss through a finite thin rectangular plate at low frequencies are compared with the results obtained by using the originally formulated MSA (Bruneau, 2006), hybrid model (FEM coupled BEM) (Sgard *et al.*, 2000) and VA One (Engineering System International [ESI], 2012), and the effects of mode-dependent radiation impedance and air loading are investigated quantitatively.

2. Numerical model

For harmonic excitation, the vibration field of the plate can be expanded on the basis of eigenfunctions ψ_{mn}, which satisfy the following equation (Bruneau, 2006)

$$\left(\frac{\partial^4}{\partial x^4} + 2\frac{\partial^4}{\partial x^2 \partial y^2} + \frac{\partial^4}{\partial y^4} - k_{mn}^2\right)\psi_{mn} = 0, \tag{1}$$

where $k_{mn}^4 = \omega_{mn}^2 M_s/B$, $B = E h^3/12(1-\nu^2)$, $M_s = \rho_p h$. B and M_s denote the bending stiffness and the mass per unit area of the plate, respectively, and ρ_p, ν, h, E are the density, the Poisson's ratio, the thickness and the Young's modulus of the plate, respectively. For the rectangular plate, simply supported, with the length a and the width b, the displacement and bending moment are zero at the boundary. If the origin of the coordinates is taken at the corner as shown in Fig. 1, the eigenfunctions and natural angular frequencies are

$$\psi_{mn} = \sin\left(\frac{m\pi x}{a}\right)\sin\left(\frac{n\pi y}{b}\right), \tag{2}$$

$$\omega_{mn} = \sqrt{\frac{B}{M_s}}\left[\left(\frac{m\pi}{a}\right)^2 + \left(\frac{n\pi}{b}\right)^2\right]. \tag{3}$$

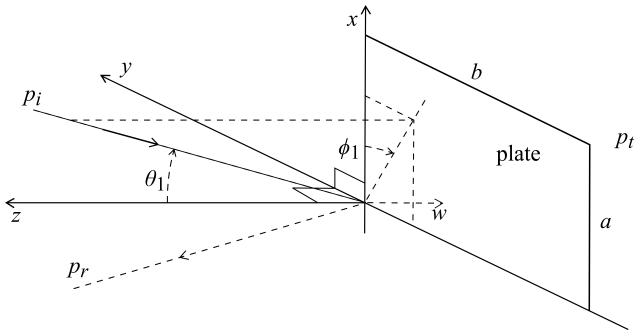

Fig. 1. Incident plane wave on a finite plate.

In Fig. 1 p_i, p_r, and p_t indicate the incident wave, the reflected wave, and the transmitted wave, respectively. ϕ_1 and θ_1 denote the polar angle and the azimuth angle, respectively.

The bending displacement of the plate $w(= We^{i\omega t})$ can be expanded as

$$W = \sum_{m,n} W_{mn}\psi_{mn}. \tag{4}$$

When the complex amplitude of the pressure p loading the plate, the equation of propagation of the bending displacement W is

$$\left[\Delta^2 - \omega^2\frac{M_s}{B}\right]W = p/B. \tag{5}$$

First, the common relationship ($\Delta^2 \equiv k_{mn}^2$) obtained from Eq. (1) and Eq. (4) is substituted into Eq. (5). Then, by multiplying the two sides of the following equation by an eigenfunction ψ_{qr} and integrating two sides with considering the orthogonal relation $\left(\iint_S \psi_{mn}\psi_{qr}\,\mathrm{d}S = \delta_{mq}\delta_{nr}\right)$, the expansion coefficient and displacement of the plate are given

$$W_{mn} = \frac{1}{B}\frac{\iint_S p\psi_{mn}\,\mathrm{d}S}{k_{mn}^2 - k_B^2}, \qquad k_B^2 = \omega\sqrt{M_s/B}, \tag{6}$$

$$W(\mathbf{r}) = \frac{1}{B}\sum_{m,n}\frac{\iint_S p(\mathbf{r}_0)\,\psi_{mn}(\mathbf{r}_0)\,\mathrm{d}S_0}{k_{mn}^2 - k_B^2}\psi_{mn}(\mathbf{r}). \tag{7}$$

The complex amplitude of the acoustic pressure on the incident side ($z > 0$) is given by

$$p_0 = p_i + p_r' - p_t, \tag{8}$$

where p_i and p_t describe the acoustic pressure amplitudes of the incident and transmitted waves, respectively, and p_r' denotes the instantaneous amplitude of the reflected pressure estimated in the case when the plate is perfectly rigid (motionless).

Since the acoustic pressure is p_t at $z < 0$ and $p_i \approx p_r'$ at $z = 0$, the complex amplitude of the total pressure loading the plate at $z = 0$ is

$$p_{z=0} = (p_i + p_r' - p_t) - p_t = 2(p_i - p_t). \tag{9}$$

The substitution of Eq. (9) into Eq. (6) leads to the expansion coefficients:

$$W_{mn} = \frac{1}{B}\frac{1}{k_{mn}^4 - k_B^4}\left[\iint_S 2p_i(\mathbf{r}_0)\psi_{mn}(\mathbf{r}_0)\,\mathrm{d}S - \iint_S 2p_t(\mathbf{r}_0)\,\psi_{mn}(\mathbf{r}_0)\,\mathrm{d}S\right]. \tag{10}$$

The leading effects of the inter-modal couplings are the shift of resonance frequencies and the increase in internal damping, while its influence on the vibrational amplitude is not severe. This is consistent with some previous researches (Takahashi, 1995; Davies, 1971), which also show that the effects of inter-modal couplings are not significant. In the often-accepted hypothesis that the transmitted pressure p_t is small compared to the incident pressure, the inter-modal coupling can be ignored (Bruneau, 2006). Thus, the transmitted pressure can be approximated as

$$p_t(\mathbf{r}_0) \approx i\,\omega \sum_{m,n} Z_{mn} W_{mn} \psi_{mn}(\mathbf{r}_0), \tag{11}$$

where Z_{mn} is the modal specific acoustic impedance.

Substituting Eq. (11) into Eq. (10) and considering the orthogonality of the eigenfunctions result in the expansion coefficients become

$$W_{mn} \approx \frac{2\iint_S p_i(\mathbf{r}_0)\psi_{mn}(\mathbf{r}_0)\,\mathrm{d}S}{2\,i\,\omega Z_{mn} - B\left(k_B^2 - k_{mn}^2\right)}. \tag{12}$$

Likewise, the substitution of Eq. (11) and Eq. (12) into the transmitted power, defined by

$$P_t = \frac{1}{2}\mathrm{Re}\iint_S p_t\,(i\omega W)^*\,\mathrm{d}\mathbf{r}, \tag{13}$$

leads to

$$P_t = \frac{\omega^2}{2}\sum_{m,n} R_{mn}\,|W_{mn}|^2 = \frac{\omega^2}{2}\sum_{m,n} R_{mn}\frac{\left|\iint_S 2p_i\,(\mathbf{r}_0)\,\psi_{mn}\,(\mathbf{r}_0)\,\mathrm{d}S\right|^2}{\left|2\,i\omega Z_{mn} - B\left(k_B^2 - k_{mn}^2\right)\right|^2}, \tag{14}$$

where $R_{mn} = \mathrm{Re}(Z_{mn})$ is the real part of the radiation impedance. Since the complex amplitude of the acoustic pressure for a harmonic incident plane wave can be expressed as $p_i = |p_i|\,e^{i(k_x x + k_y y + k_z z)}$, the transmitted power at $z = 0$ is

$$P_t = \frac{\omega^2\,|2p_i|^2}{2}\sum_{m,n}\frac{R_{mn}\,|F_{mn}|^2}{\left|2\,i\omega Z - B\left(k_B^2 - k_{mn}^2\right)\right|^2}, \tag{15}$$

with

$$F_{mn} = \iint_S e^{i(k_x x_0 + k_y y_0)}\,\psi_{mn}\,(\mathbf{r}_0)\,\mathrm{d}S. \tag{16}$$

In steady-state, where a harmonic plane wave having an angular frequency of ω is incident, the transmission coefficient τ can then be written in as

$$\tau(\omega,\theta,\phi) = \frac{P_t}{P_i} = \frac{2\rho\,cP_t}{ab\,|p_i|^2\cos\theta} = \frac{4\omega^2\rho\,c}{ab\cos\theta}\sum_{m,n}\frac{R_{mn}\,|F_{mn}|^2}{\left|2\,i\omega Z_{mn} - B\left(k_B^2 - k_{mn}^2\right)\right|^2}, \tag{17}$$

where ρ and c are the density of the surrounding fluid and the sound speed in the fluid, respectively.

The structural damping of the plate corresponds to an energy dissipation associated with various types of frictions within the material. Energy dissipation due to this type of damping can be introduced in the governing equations replacing the bending stiffness by a complex one $B \to B\,(1 + i\eta)$.

The transmission coefficient is now

$$\tau(\omega,\theta,\phi) = \frac{4\omega^2\rho\,c}{ab\cos\theta}\sum_{mn}\frac{R_{mn}\,|F_{mn}|^2}{a^*}, \tag{18}$$

where

$$a^* = M_s^2\left(\omega_{mn}^2 - \omega^2\right)^2 + \left(M_s\eta\,\omega_{mn}^2 - Ms\eta\omega^2 + 2\,\omega Z_{mn}\right)^2.$$

From the integral Eq. (16), the numerator in the summation of Eq. (18) is

$$|F_{mn}|^2 = \frac{16\,ab\pi^4 m^2 n^2}{\left(\alpha^2 - m^2\pi^2\right)^2\left(\beta^2 - n^2\pi^2\right)^2}\cdot\left[1 - (-1)^m\cos\alpha\right]\cdot\left[1 - (-1)^n\cos\beta\right], \tag{19}$$

where $\alpha = k\,a\sin\theta\cos\phi$, $\beta = k\,b\sin\theta\sin\phi$.

Now, we obtain the radiated power by calculating the sound intensity in the far field from the plate vibrating in a given mode using the Rayleigh integral and integrating it over a hemisphere over the plate. The radiation factor is therefore given as

$$\sigma_{mn} = 16k^2\pi^2 m^2 n^2 ab\int_0^{\pi/2}\int_0^{\pi/2} b^*\,\mathrm{d}\theta\,\mathrm{d}\phi, \tag{20}$$

and the real part of the specific acoustic impedance, in the (m, n) mode becomes

$$R_{mn} = 16k^2\pi^2 m^2 n^2\rho_0 c_0 ab\int_0^{\pi/2}\int_0^{\pi/2} b^*\,\mathrm{d}\theta\,\mathrm{d}\phi, \tag{21}$$

where

$$b^* = \frac{[1-(-1)^m \cos\alpha]\cdot[1-(-1)^n \cos\beta]}{(\alpha^2 - m^2\pi^2)^2 \cdot (\beta^2 - n^2\pi^2)^2} \sin\theta.$$

On the other hand, the imaginary part of the radiation impedance represents a load on the source, which, in many cases, may act as a contribution to the mechanical mass of the source. When the frequency range is below the coincidence frequency, the effective surface mass density can be employed instead of the surface mass density in vacuum, which can be written as (Zhang *et al.*, 2003)

$$M_{\text{eff}} = M_s \left(1 + \frac{\rho}{M_s\sqrt{k_f^2 - k^2}}\right), \tag{22}$$

where M_s denotes the surface mass density in vacuum and k_f is the flexural wavenumber of a plate in vacuum. k and ρ are the acoustic wave number in the surrounding fluid and the density of the fluid, respectively. According to the Eq. (22), the dependence of the mass per area of the plate on the frequency results in lowering the natural frequencies. Thus, we use the modified version of the natural frequency in Eq. (3) by including the effective surface mass density

$$\omega_{mn,\text{eff}} = \sqrt{\frac{B}{M_{\text{eff}}}}\left[\left(\frac{m\pi}{a}\right)^2 + \left(\frac{n\pi}{b}\right)^2\right]. \tag{23}$$

On real structural partitions we normally have sound incidence from many angles at the same time. We could in principle use Eq. (18), make a weighting according to the given distribution of incident angles and sum up the contributions to calculate the sound insulation. In practice, however, the actual distribution is seldom known.

When assuming an ideal diffuse incident sound field, i.e. assuming sound incidence evenly distributed over all angles and with random phase, a diffuse field transmission factor τ_d and transmission loss (TL) are calculated from the preceding expressions as bellows (Vigran, 2008):

$$\tau_d(\omega) = \frac{2}{\pi}\int_0^{\pi/2}\left[2\int_0^{\pi/2}\tau(\omega,\theta,\phi)\cos\theta\sin\theta\,\mathrm{d}\theta\right]\mathrm{d}\phi, \tag{24}$$

$$\text{TL}(\omega) = 10\cdot\log(1/\tau_d(\omega)). \tag{25}$$

3. Numerical simulation and discussion

A simply supported aluminum plate of $350\times220\times1$ mm, which is surrounded by air, is taken as an example to generate a numerical simulation. The loss factor, the density, the Young's modulus and the Poisson ratio of the plate are $\eta = 0.1\%$, $\rho = 2700$ kg/m^3, $E = 7.1\cdot10^{10}$ Pa and $\nu = 0.33$, respectively (ESI, 2012). Frequency domain for the simulation is from 10 to 500 Hz and its interval is 2 Hz.

The simulation result is compared with the ones from VA One 2012, which is an interactive software program for the analysis and design of vibro-acoustic systems, and the previous works (Bruneau, 2006; Sgard *et al.*, 2000). VA One used Statistical Energy Analysis (SEA) coupled FEM to simulate the transmission loss. Figure 2 compares the two results from VA One and Finite Element Model coupled to BEM (Sgard *et al.*, 2000).

VA One accounts for both the reactive and resistive impedance of an SEA fluid through the hybrid area junction. Two VA One models were created: in the first model both SIFs were active, in the second model one SIF was disabled. SIF is the abbreviation of Semi-Infinite Fluid, modeling the fluid in VA One. As you can see in Fig. 2, the dip position of the hybrid model (FEM-coupled BEM) and VA One is slightly different by a few hertz (somewhere around 10 Hz) and there is a noticeable difference in dip depth. This is due to the fact that the hybrid model (Sgard *et al.*, 2000) was obtained under the neglecting of the fluid loading, naturally not lowering the natural frequencies.

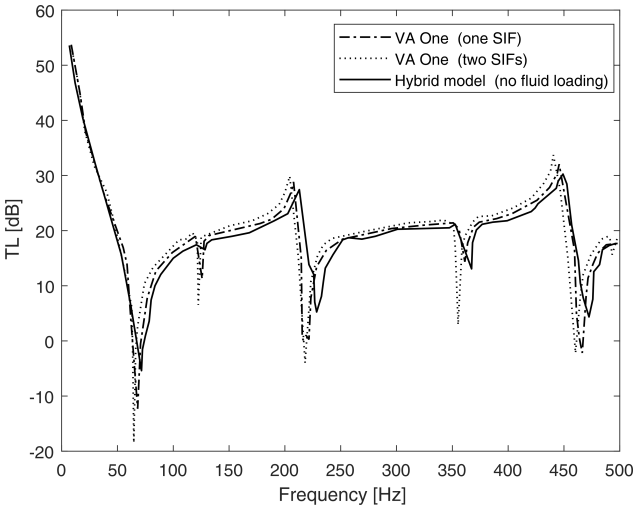

Fig. 2. TL curves from VA One and Hybrid model (FEM coupled BEM) (Sgard *et al.*, 2000).

Figure 3 shows the result from the proposed MSA model, which uses the natural frequency Eq. (3), with the ones from VA One and general MSA (Bruneau, 2006). In Fig. 3 the dips from the improved MSA model and VA One model (one SIF) match well with an average 3 dB position difference and a 3 dB depth difference. In the previous MSA model (Bruneau, 2006) the approximation $p_t(\mathbf{r}_0) \approx i\omega ZW(\mathbf{r}_0)$ has been used and the specific acoustic impedance Z has been considered equal regardless of modal number, namely $Z = \rho c$. Fluid loading has also been ignored. As a result, TL is

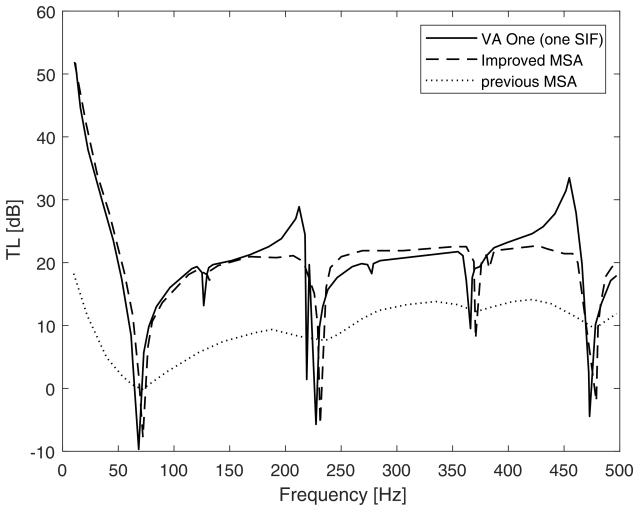

Fig. 3. TL curves from the improved MSA model, VA One, and the previous MSA model.

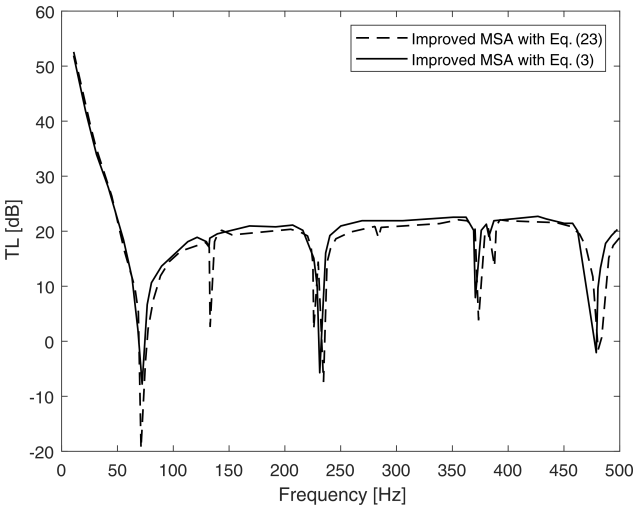

Fig. 4. The effect of the fluid loading on TL in the improved MSA model.

underestimated by more than 10 dB over the frequency range of interest. Also, in that curve, the deep dips corresponding to the natural frequency of the plate disappear.

As seen from Figs 2 and 3, the proposed MSA model, which introduces the mode-dependent specific acoustic impedance, has the unacceptable discrepancy from the VA One model with two SIFs. Figure 4 shows TL curves from the improved MSA model for two natural frequencies Eq. (23) and Eq. (3). It can be found from the figure that taking into account the influence of the fluid loading on the natural frequency, the dip in the TL curve shifts. In this case, it is 2 Hz downward. A significant change in the depth of the dips can also be observed.

Table 1 shows the positions and depths of the dips in the TL curve as well as the natural frequencies of the plate in the frequency range below 500 Hz. From the table, it is obvious that for the natural frequency modified by the added mass our MSA model becomes closer to the result from VA One with two SIFs. In this case, the average deviation between two results is 4 Hz for the dip position and 2 dB for the dip depth. As known in the past, on the other hand, the fluid loading makes the dips shifted downward from the natural frequency of the plate. And TLs at these frequencies are very small, even less than 0. The influence of odd-order mode on TL is larger than that of even-order one, especially much larger in case where the modal numbers in x- and y-direction are all odd.

The transmission losses are evaluated as a function of the loss factor for η of 0, 0.1, and 0.2%. The variation of TL with η is large around the natural frequencies, but small enough to be ignored in the rest of the ranges. Table 2 shows TL with the natural frequency and loss factor of the plate. TLs in the natural frequencies increase with increasing the loss factor, resulting in reducing the depths of dips and smoothening the curve. It can also be seen that the effect of η for the even modes is larger than that for the odd ones.

Table 1. Natural frequency of the plate and the position and depth of dips in TL curves.

No		1	2	3	4	5	6	7	8
Modal number		(1, 1)	(2, 1)	(1, 2)	(3, 1)	(2, 2)	(4, 1)	(3, 2)	(1, 3)
Natural Frequency [Hz]		71.0	131.3	223.7	231.9	284.0	372.6	384.6	478.2
VA One (one SIF)	Position of dip [Hz]	68.0	128.0	220.0	228.0	278.0	366.0	374.0	474.0
	Depth of dip [dB]	−9.9	11.8	2.4	−3.1	19.5	7.7	12.8	−2.1
VA One (two SIFs)	Position of dip [Hz]	68.0	128.0	222.0	228.0	–	364.0	372.0	472.0
	Depth of dip [dB]	−19.0	7.0	–	−3.0	–	3.5	–	−1.0
MSA (Eq. (3))	Position of dip [Hz]	72.0	132.0	224.0	232.0	284.0	372.0	384.0	478.0
	Depth of dip [dB]	−8.6	16.7	8.2	−6.1	19.7	7.5	18.3	−1.2
MSA (Eq. (23))	Position of dip [Hz]	70.0	130.0	222.0	230.0	282.0	370.0	382.0	476.0
	Depth of dip [dB]	−18.8	2.2	3.2	−6.5	19.8	3.7	13.8	−0.7

Table 2. Transmission losses as a function of the modal number and loss factor of the plate.

Natural frequency [Hz]		71.0	131.3	223.7	231.9	284.0	372.6	384.6	478.2
Mode		(1, 1)	(2, 1)	(1, 2)	(3, 1)	(2, 2)	(4, 1)	(3, 2)	(1, 3)
TL [dB]	$\eta = 0$	−19.88	−5.22	−1.14	−9.45	2.05	1.20	10.46	−2.25
	$\eta = 0.001$	−18.85	2.23	3.17	−6.53	19.74	3.73	13.77	−0.68
	$\eta = 0.002$	−17.92	6.87	6.72	−4.35	21.19	6.18	16.81	0.68

In addition to the fundamental modes, there are a number of coupled modes from Eq. (3) and Eq. (23). Due to the computational cost, it is difficult to consider the effect of all modes when calculating the TL in a given frequency or frequency range.

Figure 5 shows the modal radiation factor at frequency of 500 Hz according to Eq. (20). As shown in Fig. 5, the radiation factor has a peak for the (1,1) mode, drops into about 1/10 of the peak for some nearby modes and becomes negligible. Therefore, the modes higher than a certain threshold seldom affect TL.

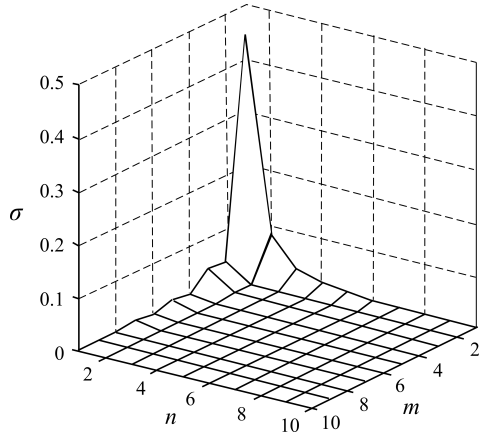

Fig. 5. Change of the radiation factor as a function of the modal number.

Figure 6 shows TLs for some frequencies as a function of upper threshold for calculation. The abscissa is the ratio of the upper threshold to the frequency of interest f_c/f and the ordinate the transmission loss normalized by its convergence. Most of curves in Fig. 6 have the horizontal regions because the natural frequencies are discrete so that the number of the vibration mode doesn't vary continuously with the frequency.

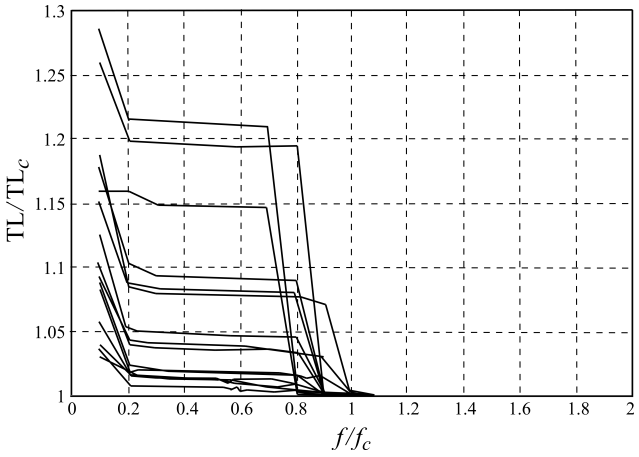

Fig. 6. Asymptotic behavior of the transmission loss with increasing the upper frequency limit.

The relative change of natural modes with frequency is much larger in the low frequency range than in the higher one. All curves in the figure approach the value of 1 at f_c/f higher than 1.1, which means that it is unnecessary to account for the contributions of the modes 1.1 times higher than the frequency of interest.

4. Conclusions

In this paper we presented an improved MSA model for estimating the transmission loss of a finite rectangular plate for diffuse field incidence in the low frequency range, in which the mode-dependent specific acoustic impedance has been introduced and the fluid loading on the plate has been taken into account as added mass.

By introducing the mode-dependent specific acoustic impedance, the accuracy of the MSA for the transmission loss prediction of the plate was improved, and the dip of the TL curve corresponding to the even mode was clearly shown.

From the simulation and comparison, it is obvious that consideration of the fluid loading in MSA leads to the more precise prediction of TL. In particular, even if it is a lighter fluid, the influence of the fluid loading in the low frequency region (below 150 Hz in this work) should be considered.

The asymptotic behaviour of TL curves was observed with the upper frequency limit to ensure both the high accuracy and low computational cost. It is found that the vibration modes ranging below 1.1 times the frequency of interest give the precise results to be acceptable.

The depth of the dips in TL curves as a function of the loss factor of the plate was discussed, which showed that even modes are affected by the loss factor more than the odd ones. In addition, the influence of odd-order modes on TL of the plate is larger than that of even-order modes and the effect gets much larger in case where the modal numbers in x- and y-direction are all odd.

Acknowledgments

The authors wish to thank the anonymous reviewers for their valuable comments, constructive remarks and suggestions to improve the quality of the paper.

References

1. Andresen K. (1999), *Underwater noise from ship hulls*, Proceedings of International Conference on Noise and Vibration in the Marine Environment, pp. 1–22, London.
2. Arenas J.P. (2003), *On the vibration analysis of rectangular clamped plates using the virtual work principle*, Journal of Sound and Vibration, **266**, 912-918.
3. Bruneau M. (2006), *Fundamentals of Acoustics*, ISTE Ltd Press, London.
4. Callister J.R., George A.R., Freeman G.E. (1999), *An empirical scheme to predict the sound transmission loss of single-thickness panels*, Journal of Sound and Vibration, **222**, 145–151.
5. Davies H.G. (1971), *Low frequency random excitation of water-loaded rectangular plates*, Journal of Sound and Vibration, **15**, 107–126.
6. Engineering System International (ESI) Group (2012), *VA One 2012, Validation and QA Document*, p. 52.
7. Fahy F. (1995), *The vibroacoustic reciprocity principle and applications to noise control*, Acustica, **81**, 544–558.
8. Fahy F., Gardonio P. (2006), *Sound and structural vibration: radiation, transmission and response*, 2nd ed., Academic Press, London.
9. Kozien M.S. (2005), *Hybrid method of evaluation of sounds radiated by vibrating surface elements*, Journal of Theoretical and Applied Mechanics, **43**, 1, 119–133.
10. Kozien M.S. (2009), *Acoustic intensity vector generated by vibrating set of small areas with random amplitudes*, Journal of Theoretical and Applied Mechanics, **47**, 2, 411–420.
11. Leppington F.G., Broadbent E.G., Heron K.H. (1982), *The acoustic radiation efficiency of rectangular panels*, Proceedings of the Royal Society of London, A 382, pp. 245–271, London.
12. Putra A., Thompson D.J. (2010), *Sound radiation from rectangular baffled and unbaffled plates*, Applied Acoustics, **71**, 1113–1125.
13. Sedov M.S. (1964), *The mechanism of transmission of a sound through a thin plate of the finite size* [in Russian], Proceedings of the Universities. Series: Construction and Architecture, No. 7, pp. 67–73.
14. Sedov M.S. (1990), *Theory of inertial sound transmission through barrier constructions* [in Russian], Proceedings of the Universities. Series: Construction and Architecture, No. 2, pp. 37–42.
15. Sgard F., Atalla N., Nicolas J. (2000), *A numerical model for the low frequency diffuse field sound transmission loss of double-wall sound barriers with elastic porous linings*, Journal of Acoustic Society of America, **108**, 2865–2872.
16. Sharp B.H. (1978), *Prediction methods for the sound transmission of building elements*, Noise Control Engineering, **11**, 53–63.
17. Takahashi D. (1995), *Effects of panel boundedness in sound transmission problems*, Journal of Acoustic Society of America, **98**, 2598–2606.
18. Vigran T.E. (2008), *Building Acoustics*, Taylor & Francis Press, London.
19. Wallace C.E. (1972), *Radiation Resistance of a rectangular panel*, Journal of the Acoustical Society of America, **51**, 946–952.
20. Xie G, Thompson D.J, Jones C.J.C. (2005), *The radiation efficiency of baffled plates and strips*, Journal of Sound and Vibration, **280**, 181–209.
21. Zhang W., Wang A., Vlahopoulos N., Wu K. (2003), *High-frequency vibration analysis of thin elastic plates under heavy fluid loading by an energy finite element formulation*, Journal of Sound and Vibration, **263**, 1, 21–46.